

Corrosion behaviour of $\text{TiN}_{0.8}\text{O}_{0.4}$ coating on 316L stainless steel alloy[†]

A. Jouaiti^{a*}, M. Boulghallat^a, L. Lâallam^a, H. Oulfajrite^a,
F. Fabreguette^b, J. Guillot^b, S. Bourgeois^b and A. Steinbrunn^b

^aLaboratoire de corrosion et de traitement des Matériaux, FST, BP 523 Beni-Mellal, Morocco

^bLaboratoire de Recherches sur la Réactivité des solides, CNRS UMR 5613, Université de Bourgogne, 9 Avenue Alain Savary, BP 47870, Dijon Cedex, France

Titanium oxinitride thin film with a thickness equal to 250 nm is obtained at 700 °C by the LP-MOCVD method. Analysis by photoelectron spectroscopy and by X-ray diffraction show that the composition of the deposit is $\text{TiN}_{0.8}\text{O}_{0.4}$ with a TiN structure. Morphological observation of the deposit, studied by scanning electron microscopy, indicated that the surface is rough with the presence of some fissures. Electrochemical study of samples in Ringer's solution (9g/l of NaCl) at 37°C, showed the role played by the surface state and imperfections on the corrosion acceleration.

Keywords: titanium oxinitride, stainless steel alloy

Among the different coating techniques used to protect metallic structures against corrosion in an aggressive environment, chemical vapour deposition and physical vapour deposition are probably the most popular.¹⁻³

Particularly, titanium compound coatings are widely used to protect the metallic structures due to their high hardness and corrosion resistance. However, several studies showed that the presence of porosity in the TiN coating on active substrate can generate an amplification of the corrosion phenomena.⁴⁻⁷ Indeed, the presence of pores in the surface and the penetration of the aggressive agent through these pores lead to the creation of a "microbattery" leading to a local acidification process. For that reason, it is necessary in the corrosion studies of the coating on an active substrate, to take into account the contribution of the latter.

In this paper we investigate the corrosion properties of TiN_xO_y thin film deposited at 700°C by low-pressure metal-organic chemical vapour deposition (LP-MOCVD) on 316L stainless steel alloy. At this temperature the phase formed is a conductrice.²

Experiment

Sample preparation: Before the development of the TiN_xO_y deposit 316L SS, the sample is polished mechanically and cleaned by ultrasounds at 70°C through the use of acetone, ethanol and trichlorométhane. The coating is realised at 700°C by low-pressure (60 torr) LP-MOCVD, the sample is placed on a graphite support heated by induction with a radio frequency system. The isopropoxide of titanium ($\text{Ti}(\text{OCH}(\text{CH}_3)_2)_4$) is used as the precursor of titanium and the oxygen. This precursor is in a liquid state at ambient temperature and at 40°C its vapour pressure is 0.35 torr. It is maintained at 40°C and is paddled by nitrogen (gas carrier). Ammonia is used as a nitrogen source.

The coating thickness is measured by scanning electron microscopy, observing the transverse section of the sample. For one hour of deposit at 700°C, the coating thickness is around 250 nm.

Characterisation methods: The structural characterisation of the films was carried out by X-ray diffraction performed on a Siemens D5000 diffractometer using a $\text{Cu K}\alpha$ radiation at 1.54 Å. The coating composition is determined with the help of a XPS apparatus equipped by a Riber spectrometer type Mac 2 and the source of X-ray used is $\text{Al K}\alpha$ radiation (1486.6 eV) with power 300 W. The electrochemical test was carried out at 37°C, in NaCl solution and the polarisation behaviour was measured potentiodynamically with a potentiostatic

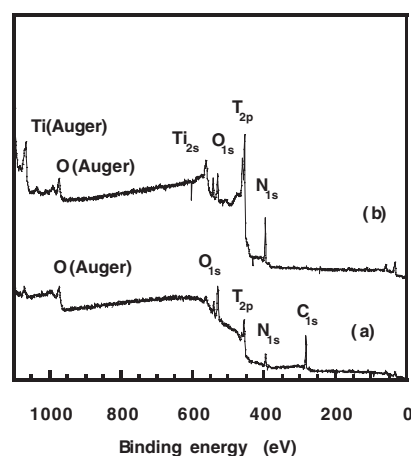


Fig. 1 XPS spectra of coating before (a) and after (b) Ar⁺ bombardment.

apparatus (Amel 2049). All potential values are given versus a saturated calomel electrode (SCE). The scanning rate was 1mV/s. The polarisation was changed from -1.2 V. Before measurements, the corrosion potential E_{cor} was monitored for 1h.

Results and discussion

The coating composition analysis by photoelectron spectroscopy: The XPS analysis has been realised after ionic bombardment in order to eliminate the contamination layer. Fig. 1 presents an XPS (photoelectron spectroscopy) spectra obtained before (Fig. 1a) and after ionic bombardment (Fig. 1b). The analysis of the initial surface state shows the presence of the titanium, the oxygen, nitrogen and carbon atoms of contamination. After five minutes of ionic bombardment, the disappearance of the carbon peak 1s, and the persistence of the characteristic peaks of the titanium, nitrogen and oxygen is observed.

In order to determine the nature of the chemical species as well as their concentration, we have recorded regions of the corresponding spectra of Ti2p, O1s and N1s with a resolution of 1.2 eV. The background was removed by a Shirley routine and desummations of spectra were done by fitting with a mixed Gaussian-Lorentzian function. The Lorentzian on Gaussian ratio was maintained constant at a value of 0.2 in all desummations. The Ti2p spectrum presented in Fig. 2, reveals two contributions. The main one, located at 455.2 eV for $\text{Ti2p}_{3/2}$ is due to the TiN_xO_y phase. The second one, at 457.6 eV, can be related to a loss peak.⁸⁻¹¹

The O1s line contains two components (Fig. 3). The main one at 531 eV corresponds to oxygen in the TiN_xO_y phase, while the contribution at 533.4 eV is assigned to the O-N bond.¹²

* To receive any correspondence. E-mail: ajouaiti@carmail.com

[†] This is a Short Paper, there is therefore no corresponding material in *J. Chem. Research (M)*.

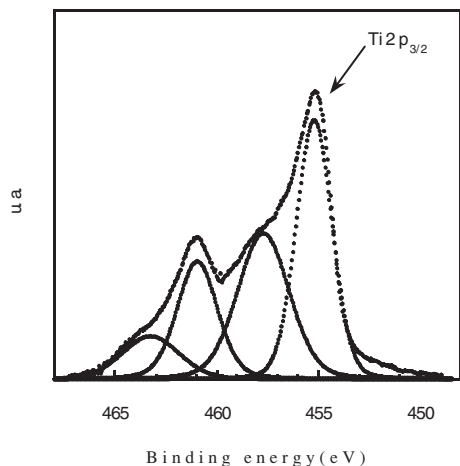


Fig. 2 XPS spectra of Ti2p line.

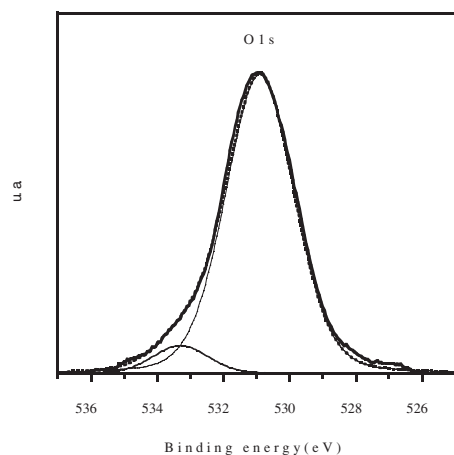


Fig. 3 XPS spectra of O1s line.

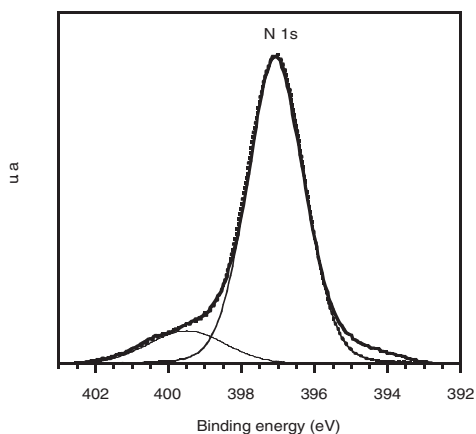


Fig. 4 XPS spectra of N1s line.

As for oxygen; the N1s spectrum (Fig. 4) contains two contributions. The main contribution at 397.1 eV corresponds to nitrogen in the TiN_xO_y phase, and the contribution at 399.5 eV is assigned to the N–O bond.¹²

Finally, the concentrations of the elements present in the coating were calculated from the XPS peaks by taking into account sensitivity factors. The values of these factors are 1.8 for Ti2p, 0.42 for N1s and 0.66 for O1s. Under these conditions the composition of the coating is: $\text{TiN}_{0.8}\text{O}_{0.4}$.

X-ray diffraction: The analysis of the film by X-ray diffraction (XRD) reveals the presence of only one crystalline phase of rock salt structure corresponding to TiN. Moreover, a shift of the XRD lines towards higher angles compared with JCPDS TiN data indicates a lattice parameter of 0.422 nm, which is smaller than that of pure TiN

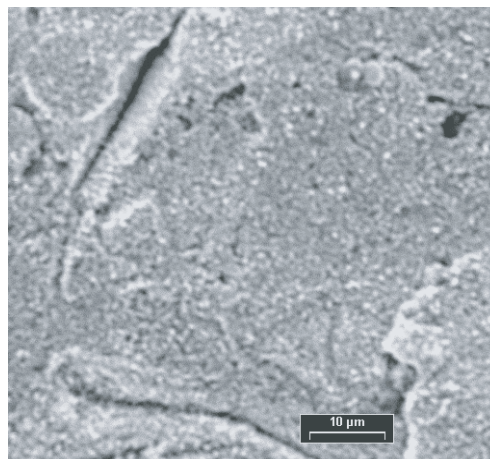


Fig. 5 SEM image of coating.

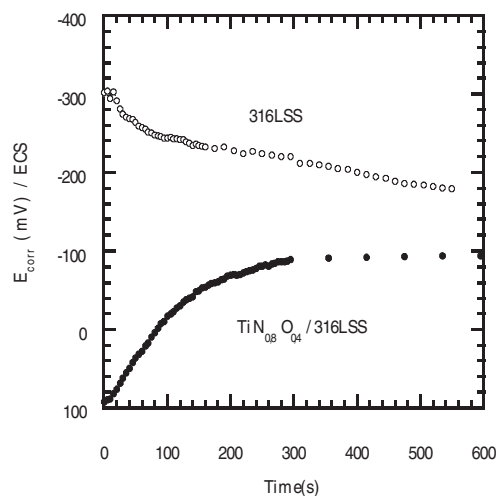


Fig. 6 Corrosion potential versus time of coated and uncoated samples.

(0.424 nm). This difference can be explained by substitution of nitrogen atoms for oxygen in the anionic sub-lattice.

Scanning electron microscopy: Observation on the deposit by scanning electron microscopy shows that the surface presents a certain roughness with some fissure (Fig. 5).

Electrochemical study: Corrosion potential measurement: The corrosion potential E_{corr} versus time curves, obtained respectively on the coated and on the uncoated samples by open circuit measurements are shown in Fig. 6. The uncoated sample curve shows that the potential increases with time from the initial potential of -302 mV/SCE to -179 mV/SCE after 10 minutes immersion. This result indicates that the passive layers of oxides or hydroxides which are formed on the surface, protect it against corrosion.

On the other hand, the coated sample curve shows that the potential decreases with time, from the initial potential of $+100$ mV/SCE to -100 mV/SCE. These evolutions indicate that the corrosion potential of the coated sample reaches the potential of the uncoated one after a long immersion time. Indeed, after 10 days of immersion, the potential value is near -133 mV/SCE, close to the uncoated corrosion potential (-115 mV/SCE) obtained after the same period of time. Such a behaviour can be explained by the fact that the coating contains pores and thus is not tight.

Intensity-potential curves: In order to study the corrosion resistance of coated and uncoated samples we have drawn the intensity-potential curves.

Fig. 7 represents the polarisation curves obtained for coated and uncoated samples in aerated aqueous NaCl solution (9g/l). One notices, that the cathodic current is nearly identical for both samples. According to the shape of the cathodic polarisation curve the kinetics of corrosion is controlled by the concentration of the oxygen in the solution. On the other hand, the analysis of the anodic polarisation curve shows that anodic dissolution is substantial near the corrosion potential for the coated sample. Under the same conditions, the

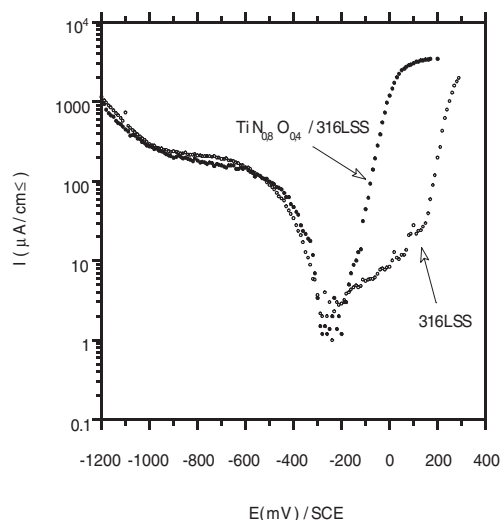


Fig. 7 Intensity-potential curves of coated and uncoated samples.

uncoated sample presents a passivation domain with a breakdown potential of 120 mV/SCE, followed by a pitting corrosion region. It results that the uncoated sample presents a better corrosion resistance than the coated one due to the passivation of the stainless steel surface which disappears in the case of the coated sample.

As it has shown in different investigations, the corrosion process of a TiN/active substrate system is controlled by the penetration of the aggressive agent through the defects in the deposit and its diffusion along the interface coating/substrate. Indeed, chloride ion has a rather large atomic radius and is weakly solvated and can therefore be adsorbed on the metallic surface. It inhibits the process of passivation responsible for the corrosion resistance. Besides, the presence of defects in the coating is the origin of crevice corrosion leading to the local acidification and consequently to an increase of the anodic current.

This observation is substantiated by other studies^{13,14} which demonstrated the aggressive role of the Cl⁻ ions towards the stainless steels in various solution. It has been shown by Nassif¹⁵ that the addition of the Cl⁻ ions in the phosphoric acid solution affects the passivity layer and induce the formation of crevice on steel 14Cr-14Ni following by the penetration of Cl⁻ through the pores or through the structures defects.

A cathodic polarisation with some millivolts (± 15 mVs) around the corrosion potential is sufficient to determine the polarisation resistance.

The polarisation resistance corresponding to each of samples is: $R_p=16.66 \text{ k}\Omega\cdot\text{cm}^{-2}$ for the 316L SS sample. $R_p=11.23 \text{ k}\Omega\cdot\text{cm}^{-2}$ for

the TiN_{0.8}O_{0.4} /316L SS sample. According to these values, one can say that the polarisation resistance of uncoated sample is heightened than the coating sample.

Conclusion

Titanium oxinitride thin film with a thickness of 250 nm is obtained at 700 °C by the LP-MOCVD method. Analyses by XPS and XRD show that the composition of the deposit is TiN_{0.8}O_{0.4} with a TiN structure. The morphological observation of the deposit by SEM, shows that the surface is rough with the presence of some fissures. Furthermore, electrochemical study of samples in Ringer's solution (9g/l of NaCl) at 37°C, demonstrated the role played by the surface state and deposit imperfections on the corrosion acceleration.

Received 3 November 2002; accepted 29 January 2003
Paper 02/1654

References

- 1 A. Giovanni, G.A. Battiston, R. Gerbasi, M. Porchia and A. Marigo, *Thin Solid Films*, 1994, **239**, 186.
- 2 F. Fabreguette, L. Imhof, M. Maglione, B. Domenichini, M.C. Marco de Lucas and P. Siblot, *Chemical Vapor Deposition* 2000, **3**, 6.
- 3 A. Bouteville, L. Imhoff and J.C. Remy, *Microelectron. Eng.* 1998, **37**, 421.
- 4 N. Vershini, K. Filonov, B. Straumal, W. Gust, I. Wiener, E. Rabkin and A. Kazakevich, *Surface Coat. Technol.* 2000, **125**, 229.
- 5 T. Valente and F.P. Galliano, *Surface Coat. Technol.* 2000, **127**, 86.
- 6 W. Brandl and C. Gending, *Thin Solid Films*, 1996, **290-291**, 343.
- 7 B. Straumal, N. Vershinin, K. Filonov, R. Dimitriou and W. Gust, *Thin Solid Films*, 1999, **351**, 204.
- 8 J. Guillot, A. Jouaiti, L. Imhoff, B. Domenichini, O. Heintz, S. Zerkout, A. Mosser and S. Bourgeois, *Surf. Interf. Analyt.* 2002, **33**, 577.
- 9 C.L. Louw, I. Le R. Strydom, K. van den Heever and M.J. van Staden, *Surf. Coat. Technol.*, 1991, **49**, 348.
- 10 I. Le R. Strydom and S. Hofmann *Vacuum*, 1990, **41**, 1619.
- 11 I. Milosev, H.H. Strehblow, B. Navinsek and M. Metikos-Hukovic, *Surf. Interf. Anal.*, 1995, **23**, 529
- 12 P.Y. Jouan, M.C. Peignon, Ch. Cardinaud and G. Lemprière, *Appl. Surf. Sci.* 1993, **68**, 595.
- 13 J.Flis, *Corros. Sci.*, 1979, **19**, 151.
- 14 N.R. Smart and T. M. Scott, *Corros. Sci.*, 1990, **30**, 877.
- 15 N. Nassif, *Surface Technol.*, 1985, **26**, 189.